Midterm Report
Jan Grzegorzewski

Reaction-Diffusion Dynamics With Fractional Brownian Motion

Summer term: 2016

Contents

List of Figures

1 Motivation

Anomalous diffusion can be observed in many different areas of nature, in particular, related to heterogeneous media like porous rocks, random resistor networks and crowded biological media with its prominent phenomena macromolecular crowding, confinement and macromolecular adsorption [10]. These environments exhibit remarkable characteristics like anomalous diffusion with its most popular power-law behaviour of the Mean-Square-Displacement ($MSD \propto t^{\alpha}$) [6], which is violating the Einstein formula $MSD = 2dDt$ and thereby the central limit theorem. Various theoretical models try to encounter the MSD power-law behaviour. These models have the main phenomenon, thus the power-law behaviour of the Mean-Square-Displacement in common, but may differ in some other observables, due to different origins of the anomalous power-law behaviour. One of these models, which are based on the phenomenon is fractional Brownian motion (fBm). It was first introduced as family of Gaussian random function by Mandelbrot and Van Ness in 1968 and motivated by examples in economics [9]. In contrast to different models of anomalous diffusion, fBm approach is plainly phenomenological focusing on the power-law of the MSD and thus perfectly qualifies as a starting point to study effects resulting from a power-law MSD.
This thesis is going to focus on fBm especially in respect to Reaction and Diffusion Dynamics. Fick's law is violated for diffusion in disordered media [5], which is essential in the derivation of the famous equation of the rate for diffusion-controlled reaction processes $k = 4\pi DR_0$. Thus, it is failing in describing reaction and diffusion dynamics while anomalous motion is present. The aim of the work is to bring diffusion-reactions dynamics and fBm together. For this purpose, an fBm integrator will be implemented into a particle-based reaction and diffusion dynamics software, which is acting on a macromolecular level. It is coarse-graining molecules into spherical particles. Usually using Brownian or Langevin motion as integrator. A fractional Brownian motion Integrator may be an elegant way of adding an approximation due to a crowded environment. The phenomenon of anomalous motion can also be studied with conventional integrators by actually building a crowded environment e.g. by adding obstacles. Nevertheless, the fBm approach could save computational time since it is not necessary to simulate each particle explicitly, which builds up the crowded environment. Furthermore different studies show that heterogeneous environments have influences on particle segregation in the presence of reactions [1], which is an interesting phenomenon of self-organization.

Having an Introduction set, chapter 2 deals with the theoretical foundation for fBm. Subsequently, due to computational reasons these theoretical elaborations need to be transferred into discrete space and finally casted into an algorithm. In the following some properties of the algorithm are studied. In Chapter 3, the theoretical foundation for reactions is going to be set. Results from a reaction-diffusion simulation (with ReaDDy) without fBm will be shown. Similar setups will deal as a reference for later simulations with fBm.

2 Theory

2.1 Basics

Fractional Brownian motion is a more general family of Gaussian random function than standard Brownian motion. The following section will explore in more detail the theoretical foundation for Brownian motion and normal diffusion. After acquiring the required knowledge also the more general case of fBm will be studied.
Standard Brownian Motion is a very important and good studied stochastic process. It describes the erratic motion of mesoscopic particles, which first were documented by Jan Ingenhousz in 1785, in particular for coal dust on the surface of alcohol[6]. Later on, in 1827 Robert Brown observed the erratic motion of pollen grains. Brownian Motion has a Gaussian propagator, which has its origin in the Central Limit Theorem (CLT) for a sum of independent and identically distributed random variables. Let's assume a set of N independent variables $\{X_i\}$ with a finite variance $\sigma_i^2 = \langle X_i^2 \rangle$ and the mean $\langle X_i \rangle = 0$. The definition of an another random variable Y is given by:

$$Y = \frac{1}{\sqrt{N}} \sum_{j=1}^{N} X_j \tag{2.1}$$

This scenario in which a random variable is defined by the sum of another can be observed generically in nature. The seemingly innocent assumption of independence for the random variable $\{X_i\}$ in the summation results in the limit of large N $\rho(y)dy = P(y < Y < y + dy)$ in a Gaussian distribution $\rho(y)$

$$\rho(y) = \frac{1}{\sqrt{2\pi}\sigma} e^{-\frac{y^2}{2\sigma^2}} \tag{2.2}$$

A calculation of this very interesting result can be found in the appendix 4.1. Microscopic processes, which result in independent random position changes of a particle and add up over time, thus have a Gaussian distribution function for the overall change in position. With Bayes' theorem and an initial delta-distribution one can show that transition probability $T_t(y|0) = \rho_t(y)$ is equivalent to the particle density distribution. One can find the calculation in the appendix 4.2. The above-mentioned elaborations motivate the reason for a process with a Gaussian transition probability and standard Brownian motion has a Gaussian distributed transition probability.

2.2 Brownian motion

Definition 1 *Standard Brownian motion is a stochastic process* $\{W_t\}_{t\geq 0} : \Omega \to \mathbb{R}^d$ *with* $W_t(\omega)$ *being the position of a particle with* $\omega \in \Omega$ *at time* $t \in T$ *in the observation time* $T = [0, \infty)$*. It has a fixed* $x \in \mathbb{R}^d$ *as its origin. The transition probabilities are [3]:*

$$T_t(y|x) := (2\pi t)^{-\frac{d}{2}} e^{-\frac{||x-y||^2}{2t}} \text{for } y \in \mathbb{R}^d, t > 0 \qquad (2.3)$$
$$T_0(y|x) = \delta(x-y)$$

In the following some properties of Brownian motion are discussed:

- Brownian motion is a Gaussian process with mean $E^x[W_t] = x$, $W_o = x$. Since $E^x[(W_{t_i} - W_{t_{i-1}})(W_{t_j} - W_{t_{j-1}})] = 0$ all its increments $\{W_{t_1}, W_{t_2} - W_{t_1}, ..., W_{t_k} - W_{k-1}\}$ are independent.
- Brownian motion has stationary increments since $W_{t-h} - W_h$ has the same distribution for all $h > 0$.
- Brownian scaling $\{\hat{W}_t := \frac{1}{c} W_{c^2 t}\}_{t\geq 0}$ if $\{W_t\}_{t\geq 0}$ is also a Brownian motion. Therefore Brownian motion has self-similar and fractal paths.

Now introducing Fick's second law of diffusion. It predicts how diffusion causes the concentration to change over time:

$$\frac{\partial}{\partial t} c(\boldsymbol{r}, t) = -\nabla J(\boldsymbol{r}, t) = D\Delta c(\boldsymbol{r}, t) \qquad \text{with} \qquad \Delta = \nabla^2 \qquad (2.4)$$

With Fick's first law $-J(\boldsymbol{r}, t) = \nabla c(\boldsymbol{r}, t)$ and D being the flux of particles and the diffusion coefficient, respectively. Fick's first law is a result from the linear response theory. Fick's second law can be derived from the continuity equation and Fick's first law. The Concentration $c(\boldsymbol{r}, t)$ can be interpreted as a probability distribution, if properly normalized $\int d\boldsymbol{r} c(\boldsymbol{r}, t) = 1$. For further calculation the mathematical description of a transition probability of Brownian motion will be replaced with a more physical description of a propagator:

$$P(\boldsymbol{r}, t) = \left(\frac{2\pi\delta\boldsymbol{r}^2(t)}{d}\right)^{-\frac{d}{2}} e^{-\frac{\boldsymbol{r}^2 d}{2\delta\boldsymbol{r}^2(t)}} \qquad (2.5)$$

One can show that the propagator is solving eq. (2.4) with $\delta\boldsymbol{r}^2(t) = 2dDt$ and the meaningful initial condition of vanishing concentration at boundaries:

$$c(\pm\infty, t) = 0 \qquad (2.6)$$

The calculation can be found in the appendix 4.3. For further references, a scale-free form of the Gaussian propagator will be introduced. It is a more intuitive

consequence of Brownian scaling.

$$P(\boldsymbol{r},t) = r^{-d}\mathcal{P}_{gauss}(\hat{\boldsymbol{r}}) \qquad \text{with} \qquad \hat{\boldsymbol{r}} = \frac{\boldsymbol{r}}{\sqrt{2Dt}} \tag{2.7}$$

2.3 Fractional Brownian Motion

In this section the theoretical foundation for fractional Brownian motion will be set and related to standard Brownian Motion.
In the previous section the MSD has been shown to be linear with time as a result of the central limit theorem. In normal liquids this behaviour can be seen already at time scales higher than picoseconds [6]. Nevertheless, many experiments show that the MSD has a power law behaviour ($\delta r^2(t) \propto t^\alpha$ for $0 < \alpha < 1$). Thus, the central limit theorem does not hold, not even for long time scales. It can be shown that persistent correlations of the increments are present. In soft matter, like polymers,a subdiffusive behaviour is typically present in a time window but finally the linear MSD takes over. Fractional Brownian motion instead examines the case that the central limit theorem is violated for all time scales. The basic feature of fBm's is that the "span of interdependence" between their increments can be said to be infinite[9]

Definition 2 *Just like standard Brownian motion, fBm is a Gaussian process* $\{X_t\}_{t\geq 0} : \Omega \to \mathbb{R}^d$. *Therefore it is fully specified by its mean* $E[X_t] = 0$ *and its (co)variance function* $Cov[X_t, X_s] \overset{stationary}{=} C(t-s) = E[\delta X^*_{t-s} X_0] \propto t^\alpha$.

In terms of anomal diffusion fBm's variance can be written as:

$$\delta r^2(t) =< \Delta R(t) >= 2dK_\alpha t^\alpha \tag{2.8}$$

with $K_\alpha > 0$ being the generalized diffusion coefficient.
In the following some properties of fBm will be discussed:

- The single particle density $\rho(\boldsymbol{r},t) = \delta(\boldsymbol{r} - \boldsymbol{R}(t))$ describes the density of a particle, which is localized at position $\boldsymbol{R}(t)$. Its correlation function $P(\boldsymbol{r} - \boldsymbol{r}', t - t') = V\langle\rho(\boldsymbol{r},t)\rho(\boldsymbol{r}',t')\rangle$ is also called Van Hove self-correlation function (in this context the propagator). V refers to the volume. From now on we will consider an isotropic system $r = |\boldsymbol{r}|$. As for Brownian motion with independent increments the correlated increments $\Delta R(t)$ of fractional Brownian motion are assumed to follow a Gaussian distribution with zero mean. Thus the correlation function of the single particle density results in:

$$P(r,t) = [2\pi\delta r^2(t)/d]^{-\frac{d}{2}} e^{\frac{-r^2 d}{2\delta r^2(t)}} \tag{2.9}$$

- The propagator of fBm can be transformed into a scale free form. It is related

to the scale free from of standard Brownian motion eq. (2.7):

$$P(\boldsymbol{r},t) = \boldsymbol{r}^{-d}\mathcal{P}_{gauss}(\hat{\boldsymbol{r}}) \qquad \text{with} \qquad \hat{\boldsymbol{r}} = \frac{\boldsymbol{r}}{\sqrt{2K_\alpha t^\alpha}} \tag{2.10}$$

- The van hove correlation function can be transformed via the spatial Fourier transform into its wave-number representation, which is called the self-intermediate scattering function. Again for isotropic systems one can write $|\boldsymbol{k}| = k$.

$$F_s(k,t) = \langle \rho(k,t)\rho(k',t')\rangle = \int d^d r e^{-ikr} P(r,t) \tag{2.11}$$

$$= \langle e^{-ik\Delta R(t)}\rangle \tag{2.12}$$

- The intermediate scattering function for the single particle density turns out to be the characteristic or moment generating function of $\Delta R(t)$ by expanding it for small wavenumbers $k \to 0$ one can get the moments. Its logarithm returns the cumulants. For Gaussian propagators with zero-mean all but the second cumulants vanish. For non-Gaussian transport also further cumulants are non-zero. Therefore, it is used to indicate beyond Gaussian transport. The non-Gaussian parameter is defined as:

$$\alpha_2 = \frac{d\delta r^4(t)}{(d+2)[\delta r^2(t)]} - 1 \tag{2.13}$$

- An other important quantity is the dynamical structure factor, which is the time-frequency Fourier transform of the intermediate scattering function:

$$F_s(k,z) = \langle \rho(k,z)\rho(k',z')\rangle = \int_0^\infty dt e^{-itz} P(k,t) \text{ for } k \to 0, \mathrm{Im}(z) > 0 \tag{2.14}$$

$$= \frac{1}{-iz} - \frac{k^2}{2d}\int_0^\infty dt e^{izt}\delta r^2(t) + \mathcal{O}(k^2) \tag{2.15}$$

From now on lets start from velocities as our random variables $\partial_t \boldsymbol{R}(t) = \boldsymbol{\xi}(t)$. $\boldsymbol{\xi}(t)$ are velocities, which are no more delta-correlated in time as they would be for standard Brownian motion.

- Velocities can be used to calculated the Velocity Autocorrelation Function (VACF):

$$Z(|t-t'|) = \frac{1}{d}\langle \boldsymbol{\xi}(t)\boldsymbol{\xi}(t')\rangle = \frac{1}{2d}\frac{d^2}{dt^2}\delta r^2(t-t') \tag{2.16}$$

The VACF in the frequency domain for fBm is:

$$\tilde{Z}(z) \overset{\mathrm{Im}(z)>0}{=} K_\alpha \Gamma(1+\alpha)(iz)^{1-\alpha} \tag{2.17}$$

The calculation can be found in the appendix 4.4

Eventually, the VACF in the frequency domain will be used to modify standard Brownian motion velocities, which are easily computable, to generate fractional Brownian motion velocities. The starting point are the velocities $\partial_t \boldsymbol{R}(t) = \boldsymbol{\xi}(t)$. The increments can be decomposed in its Fourier modes for real frequencies $z = \omega$:

$$\tilde{\boldsymbol{\xi}}_T(\omega) = \int_{-\frac{T}{2}}^{\frac{T}{2}} dt e^{i\omega t} \boldsymbol{\xi}(t) \tag{2.18}$$

For a finit observation time T the Wiener-Khinchin theorem applies :

$$\lim_{T\to\infty} \frac{1}{T} \langle |\tilde{\boldsymbol{\xi}}_T(\omega)|^2 \rangle = 2\,\mathrm{Re}\left(\tilde{Z}(\omega)\right) \tag{2.19}$$

For white noise one gets:

$$\lim_{T\to\infty} \frac{1}{T} \langle |\tilde{\boldsymbol{\eta}}_T(\omega)|^2 \rangle = const. \tag{2.20}$$

Fractional correlations can be incorporated via its VACF:

$$\tilde{\boldsymbol{\xi}}(\omega) = \sqrt{2\,\mathrm{Re}\left(\tilde{Z(\omega)}\right)}\tilde{\boldsymbol{\eta}}(\omega) \tag{2.21}$$

With $\tilde{\boldsymbol{\xi}}(\omega)$ being fractional Brownian velocities in the frequency domain. Its Fourier-back-transform results in fractional Brownian velocities in the time domain.

$$\boldsymbol{\xi}(t) = \int d\omega e^{i\omega t} \tilde{\boldsymbol{\xi}}(\omega) \tag{2.22}$$

2.3.1 Algorithm

In the following an algorithm, which generates fractional Brownian noise will be introduced. The algorithm is based on the Davis-Harte algorithm [2]. The idea is to use the calculated VACF and thereby modify conventionally generated Gaussian random variables. All the increments should be generated beforehand. With this concept, it is more difficult to include forces. Nevertheless, it is computationally favourable than computing each increment recursively considering also its history. This can be done by the exact algorithm of hosking [7]. This would be certainly necessary since all increments are defined to be more than just delta-correlated in time. For computational reasons the elaborations for fractional Brownian motion in the previous chapter on how to generate fractional Brownian increments have to be transformed into a discrete form, thereby the solution is no longer exact, which will be shown in the analysis part of the algorithm.

$$\boldsymbol{\eta}(t) \longrightarrow \boldsymbol{\eta}_j(t) \text{ with } j = 0, 1, 2, ..., n \text{ , } n = \text{amount of steps} \tag{2.23}$$

For a n-steps long trajectory one can write:

$$\Delta \boldsymbol{R}_n(t) = \sum_{j=0}^{n} \boldsymbol{\eta}_j \Delta t \tag{2.24}$$

The following algorithm is explained for one dimension and can be easily extended for more dimensions. The MSD then can be written as:

$$< \Delta R_j(t) >= 2K_\alpha(\Delta t j)^\alpha \tag{2.25}$$

The algorithm goes as follows:

1. M independent normally distributed random increments are generated:

$$\eta_k(t) = \mathcal{N}(0, \sqrt{\Delta t}) \text{ with } k = 0, 1, 2, ..., M \tag{2.26}$$

   $M > n$ more increments are generated to counteract the boundary problem in the discrete Fourier transform, which is shown in fig. 2.1 and fig. 2.2

2. Via discrete Fourier transform these increments are transformed into the frequency domain:

$$\tilde{\eta_l}(z) = \sum_{k=0}^{M-1} \eta_k e^{\frac{-i2\pi lk}{M}} \Delta t \text{ with } l = 0, 1, 2, ..., M \tag{2.27}$$

$$\tag{2.28}$$

   By comparison with the eq. (2.18) one can see that:

$$z \to l\Delta z \ , \ \Delta z = \frac{2\pi}{M\Delta t} \ , \ t \to j\Delta t \text{ and } \int dt \to \sum \Delta t \tag{2.29}$$

3. Comparable to eq. (2.21) correlations are incorporated:

$$\tilde{\xi}_l(z) = \tilde{\eta}_l(z)\sqrt{2Re(\tilde{Z}_l(z))} \tag{2.30}$$

   with $\tilde{Z}(z) \to \tilde{Z}_l(z)$ as introduced in eq. (2.29):

$$\tilde{Z}_l(z) = K_\alpha \Gamma(1+\alpha)(i2\pi l\Delta z)^{1-\alpha} = K_\alpha \Gamma(1+\alpha)(il\frac{2\pi}{M\Delta t})^{1-\alpha} \tag{2.31}$$

4. The discrete Fourier transform has a downside compared to the continuous Fourier transform, as already noted in the beginning of this section. The VACF is zero at zero-frequency $\tilde{Z}_{l=0}(z=0) = 0$. From eq. (2.30) also the first increment in the frequency domain is zero $\tilde{\xi}_{l=o}(z=0) = 0$. Due to eq. (2.27)

also the following relation holds:

$$\tilde{\xi}_{l=o}(z) = \sum_{k=0}^{M-1} \xi_k e^0 \Delta t = \Delta R_M \tag{2.32}$$

ΔR is the distance between the starting point and the position of the particle. Therefore, the particle would travel after M steps back to its initial position. The effect on the ensemble averaged mean square displacement can be seen in fig. 2.1. Instead, the zero-increment in the frequency domain is calculated as follows:

$$\tilde{\xi}_{l=o}(z) = \mathcal{N}(0, \sqrt{2K_\alpha(M\Delta t)^\alpha}) \tag{2.33}$$

This equation would be correct if we assumed fractional Brownian motion

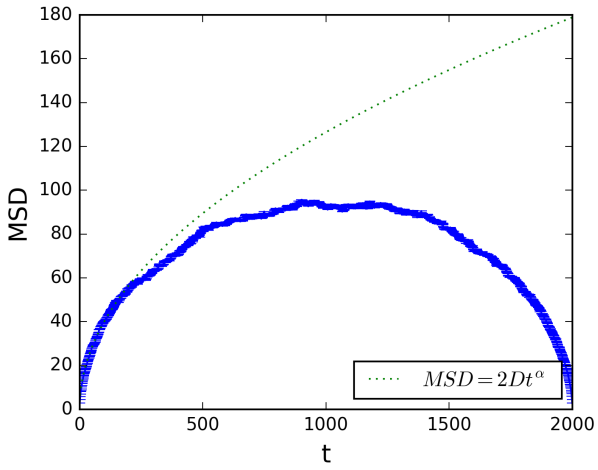

Figure 2.1: Ensemble MSD without the correction introduced in eq. (2.32)

to be a Markovian process, which certainly is not the cause. This is also the reason why M have been chosen to be bigger than n. The presumption is, that the impact of the approximation would be negligible with increasing distance to ΔR_M and negligible at ΔR_n. The impact on the ensemble averaged MSD can be seen in fig. 2.2. This can be thought of as a finite-time correction.

5. With the reverse Fourier transform the fractional Brownian noise increments in the time domain result in:

$$\xi_k = \frac{1}{2n} \sum_{l=0}^{2n-1} \tilde{\xi}_l e^{\frac{2\pi i l k}{2n}} \Delta z \tag{2.34}$$

Only n increments are taken into account ξ_j for $j = (0, 1, .., n)$.

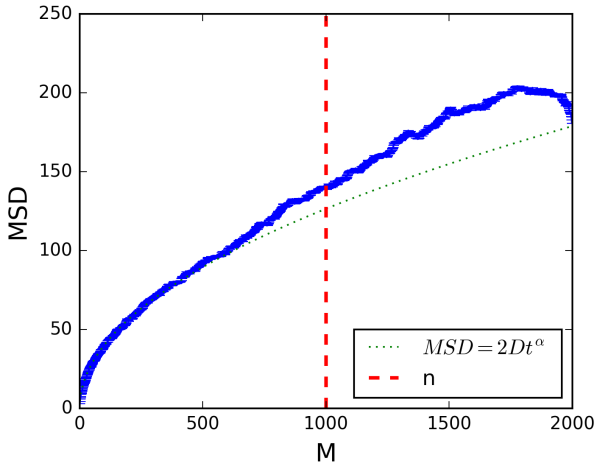

Figure 2.2: Ensemble MSD with correction introduced in eq. (2.32). The side of the red bar indicates the threshold for the remaining increments for $M = 2n$

The described algorithm can be performed for every Cartesian component of the three dimensional fractional Brownian motion. The Cartesian component are not correlated.

Testing of the Algorithm

The algorithm is implemented in python and c++. For the c++ implementation a wrapper to python is added. Both algorithms have been analysed by an analysis class. The c++ implementation is using FFTW library for the Fast Fourier Transform and Mersenne-Twister (gsl_rng_mt19937) as the random number generator. The algorithm is intended to be integrated into a **Rea**ction **D**iffusion **Dy**namics package (ReaDDy). A new c++ version of ReaDDy is currently developed. The algorithm is meant as an integrator for the particles additionally to normal Brownian motion and Langevin. The python implementation was developed beforehand and will no longer be developed but only serves as a reference. Python uses the numpy.fft library for the Fast Fourier Transform and also the Mersenne-Twister random number generator.
To get insight into the stochastic algorithm one has to study observables, which are generally averaged values. The algorithm was designed to produce fBm. The most important quantity is the variance i.e. MSD. It can be calculated as the ensemble-, time- or time-ensemble-average. It is shown in fig. 2.3 . Comparing time and ensemble averages are showing no violation of ergodicity. The tails of the time and ensemble-time averages are starting not to follow the theoretical values due to decreasing statistics. In the following figures ensemble averages have been chosen. They are computationally cheaper. It can be seen, that the algorithm tends to result in too MSDs for small lag times. This is caused by the finite amount of samples in the discrete Fourier transform until know reducing these effects is only possible

by reducing the time step.

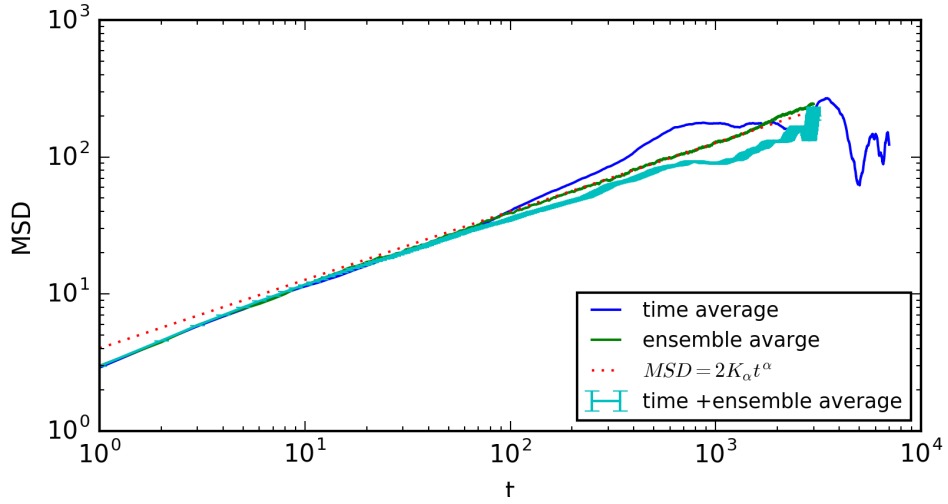

Figure 2.3: Comparison of Mean-Square-Displacements between time-average, ensemble-average and time-ensemble-average for $D = 2$, $\alpha = 0.5$, $\Delta t = 1$. For the time ensemble average only 10 trajectories have been taken.

The influence of the time step size is shown in fig. 2.4 . The deviation from the expected value is linearly dependent on the amount of samples in the interval. Another

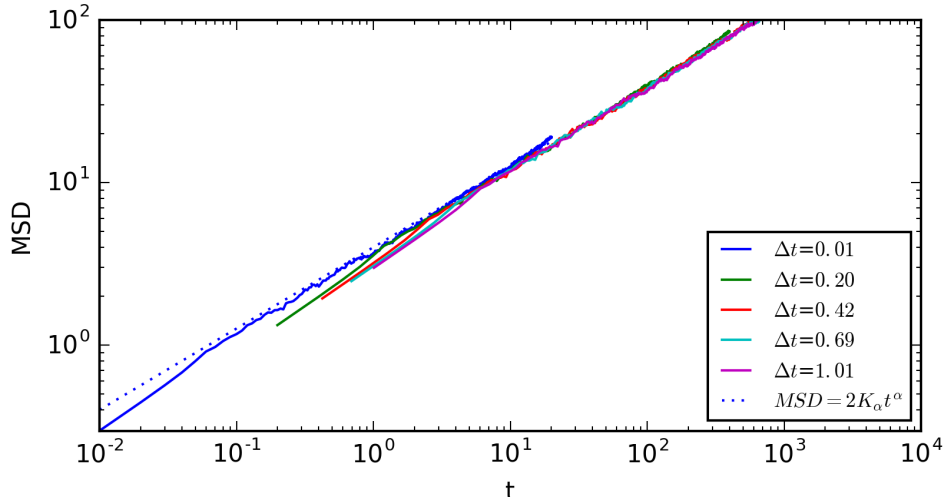

Figure 2.4: Comparison of ensemble averaged Mean-Square-Displacements with different Δt for $D = 2$, $\alpha = 0.5$.

MSD influencing variable is the anomalous coefficient α. The influence on the MSD is shown in fig. 2.5 . In the limit of Brownian motion $\alpha = 1$ the artifacts for small lag-times vanish. The downside are longer simulation times for the same time in the

simulation. The generalized diffusion coefficient has also bin varied. The influence

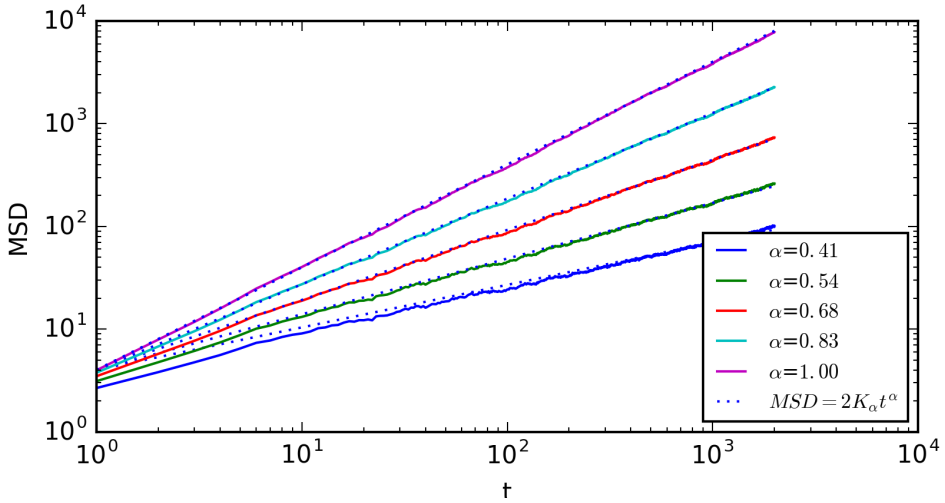

Figure 2.5: Ensemble averaged MSD for different α with $K_\alpha = 2$, $N = 2000$, $n = 2000$, $\Delta t = 1$, $M = 2n$.

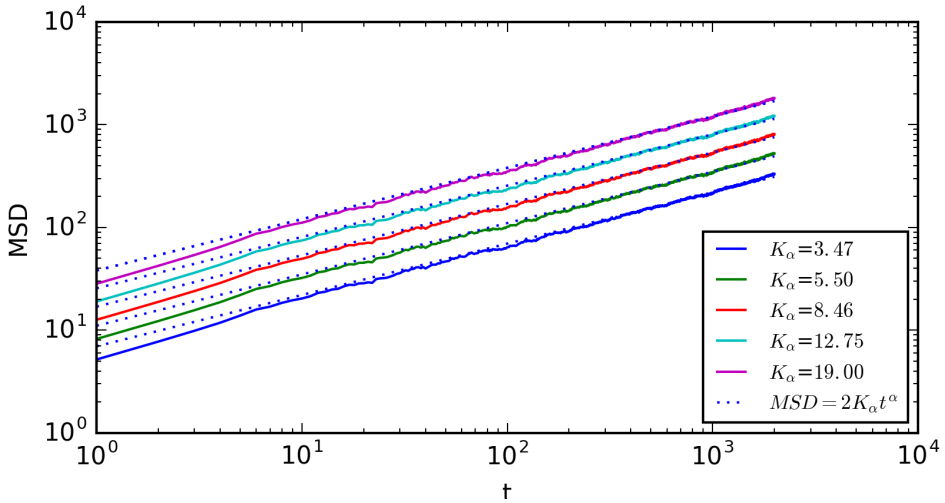

Figure 2.6: Ensemble averaged MSD for different K_α. with $\alpha = 0.5$, $N = 2000$, $n = 2000$, $\Delta t = 1$, $M = 2n$.

on the MSD can be seen in fig. 2.6 . The change of K_{alpha} is not influencing the quality of the simulation. As a property of self similarity a scale free version of the density distribution can be calculated section 2.3 eq. (2.10). The scale free density distribution is not depended on time but overlaps for all times. The algorithm is performing as predicted and computing a self-similar process. The scale free distribution is extracted from the simulation for different times and compared to the

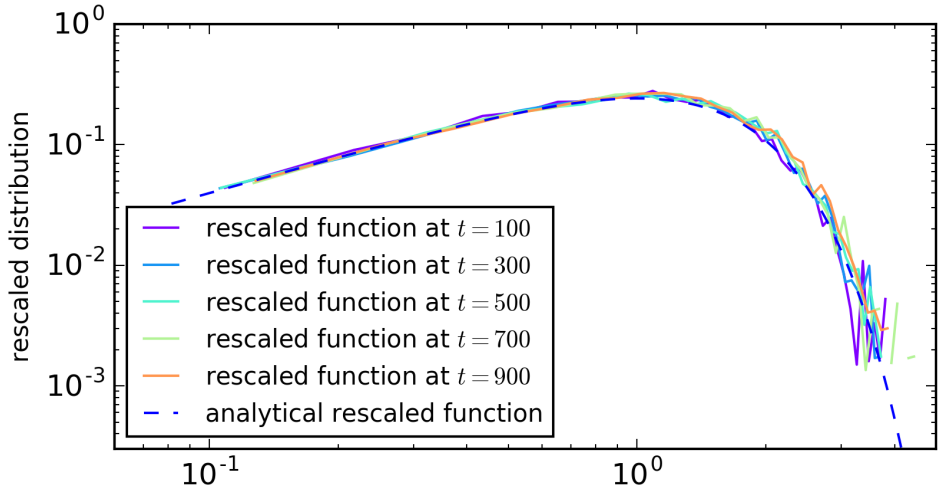

Figure 2.7: The scale free form of the Propagator at different times as introduced in eq. (2.10). With $K_\alpha = 2$, $\alpha = 0.5$, $N = 10000$, $\Delta t = 1$, $M = 2n$.

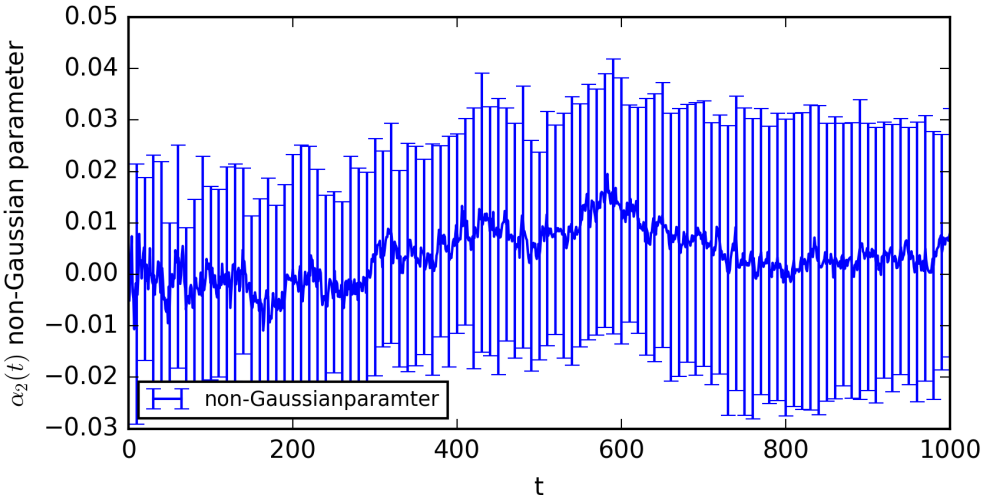

Figure 2.8: Non-Gaussian-Parameter (as introduced in eq. (2.13)) With $K_\alpha = 2$, $N = 5000$, $n = 1001$, $\Delta t = 1$, $M = 2n$ averaged over 30 non-Gaussian-Parameter with its variance displayed as an error bar.

analytical result. The graph can be seen in fig. 2.7. Subsequently also the non-Gaussian parameter was analyzed. For a perfect Gaussian process it should be zero as it is shown in eq. (2.13).
Finally the algorithmic scaling was tested. FFT in python and c++ should scale for large number as $\mathcal{O}(Mlog(M))$, which seams to be the cause for this algorithm as one can see in fig. 2.9. Further also the computational time(t) dependence on trajectories (N) were profiled as one can see in fig. 2.10.Again $t = M^{0.7}$ for large N.

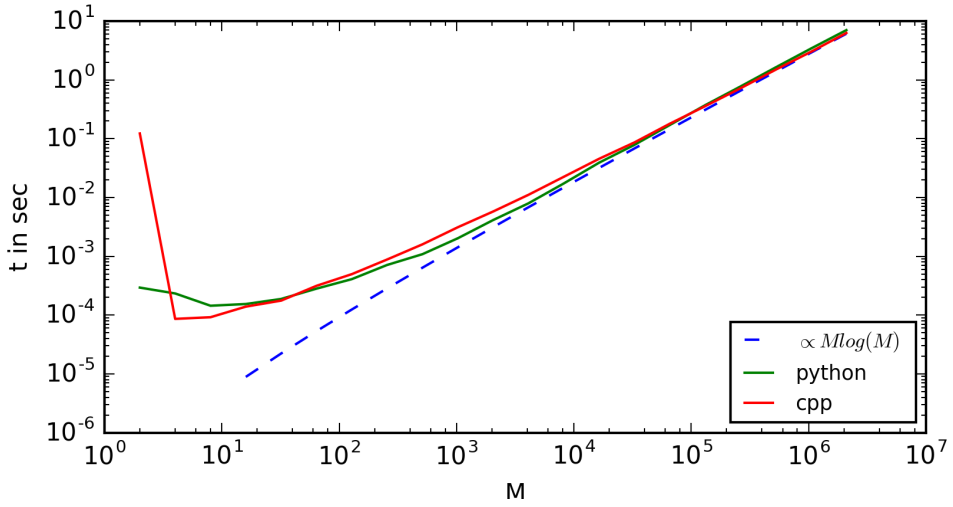

Figure 2.9: Profiling c++ and python code in respect to trajectory length M,for $N = 1$, $t = \mathcal{O}(Mlog(M))$

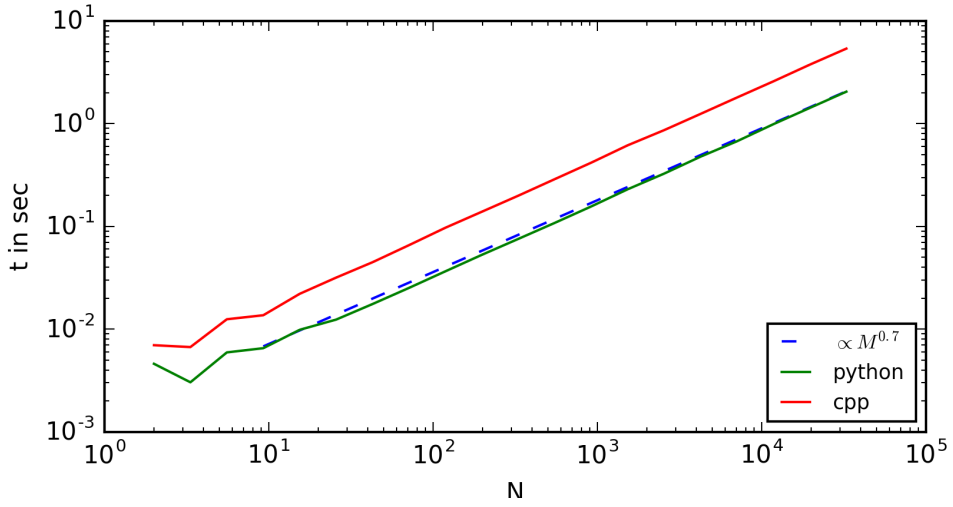

Figure 2.10: Profiling c++ and python code in respect to trajectory number N for $M = 1000$,$t = \mathcal{O}(Nlog(N))$

3 Reactions-Diffusion-Dynamics

3.1 Theory

3.1.1 Diffusion-controlled Reactions for Brownian Motion

Chemical reactions are omnipresent in biological systems. Reactions are composed of reactants and products. These reactants and products are atoms or molecules with changing number over time during reactions. Studying chemical reactions often contains reaction kinetics. Reaction kinetics is about rates of chemical process. Enzymatic reactions e.g. play an important role in biological systems to reduce rates of reactions. The rates of reactions in solutions are not only governed by intrinsic reaction rates, which were addressed e.g. by Kramer's escape problem for two reactants, but also on rates at which the chemical participants diffuse into close proximity. In a reaction of the following type: $\mathrm{A} + \mathrm{B} \underset{k_\mathrm{d}^-}{\overset{k_\mathrm{d}^+}{\rightleftharpoons}} \mathrm{AB} \underset{k_\mathrm{a}^-}{\overset{k_\mathrm{a}^+}{\rightleftharpoons}} \mathrm{C}$.
The Kramer's escape problem deals with the rates on the right side $k_\mathrm{a}^{\pm}$. Smoluchowski deals with the rates on the other side $k_\mathrm{d}^{\pm}$.
A theoretical approach on how fast two particles come together in a dilute system of hard spheres moving independently with Brownian motion have been studied by Marian von Smoluchowski in 1916 [12]. This was the first study on diffusion-limited reaction rates. A constant rate k^+ can be written as:

$$k^+ = 4\pi(D_1 + D_2)(R_1 + R_2) = 4\pi(D_1 + D_2)\sigma \tag{3.1}$$

with $\sigma = R_1 + R_2$ the relative distance between the sphere centres. It is a direct result of the diffusion equation. The calculation can be found in the appendix 4.5.
One particular area of research on which the Smoluchowski relation had significant impact in the last few decades is biology. This is unsurprising as a vast number of biomolecular systems involve dilute and minute diffusing molecular populations undergoing continuous reaction. Understanding how these biological systems operate is complicated and is in itself a whole field of research; systems biology. The Smoluchowski result has provided a very powerful tool for theoretical investigation of microscopic biochemical reaction-diffusion processes [4]. It was extended by P. Debye in 1942 to add intermolecular forces. However, especially in biological systems Brownian motion do not apply for all time-scales. As stated in the motivation these environments exhibit very often anomalous diffusion, which can be addressed by fBm.
A related reaction type was studied by L. Michaelis and Maud L. Menten in 1913 [8]. Also Known as Michaelis-Menten kinetics: $\mathrm{S} + \mathrm{E} \underset{k_1'}{\overset{k_1}{\rightleftharpoons}} \mathrm{ES} \underset{k_2'}{\overset{k_2}{\rightleftharpoons}} \mathrm{P} + \mathrm{E}$, with

$k_2' = 0$. The assumption of irreversibility can be considers as a good approximation, if the concentration of the substrate is a lot larger then the concentration of the Product $[S] \gg [P]$ or if the Gibbs free energy (released energy) is very large $\Delta G \ll 0$ (Kramer's escape Problem). With a further quasi-steady-state approximation ($k_1[E][S] = k_1'[ES] + k_2[ES]$) the Michaelis-Menten equation results in:

$$v = \frac{d[P]}{dt} = V_{max}\frac{[S]}{K_M + [S]} \qquad \text{with} \qquad K_M = \frac{k_1' + k_2}{k_1} \tag{3.2}$$

The derivation can be found in the appendix 4.6 . In the first step the relation $\frac{d[ES]}{dt} \propto [E][S]$ is assumed. This is coherent with the results from the calculation for kinetics of bi-molecular reaction in solutions with the assumption of normal diffusion in section 4.5. However, in the environment of a living cell where there is a high concentration of proteins, the cytoplasm often behaves more like a gel than a liquid, limiting molecular movements and altering reaction rates [13].

3.2 Simulation and Outlook

A software package revReaDDy was used to simulate reactions in a dilute system. It builds upon ReaDDy [11] and is still under development. It is a particle based simulation software acting on a macromolecular level. For the following simulation Brownian motion was used as an integrator and will be replaced by fBm in the second half of the master thesis. RevReaDDy has periodic boundary conditions. In the following, possible input parameters will be mentioned. Particle types with a radius and diffusion constant can be defined. Further, also the simulation box size can be varied. Different types of reactions can be incorporated. Their parameters are: 1. Intrinsic reaction rates k_a: They describe the speed of the reaction as soon as the reactants are in a close proximity. 2. The distance for close proximity. 3. Which particles take part in the reaction.
In the following, results from an enzymatic reaction will be shown. The reaction is a simplified version of Michaelis-Menten. That is what we intended to simulate. Formation of complexes is still not integrated in revReaDDy. A close reaction scheme to Michaelis-Menten can be reduced to: $\mathrm{S} + \mathrm{E} \xrightarrow{k_1} \mathrm{P} + \mathrm{E}$. This kind of reaction type is already integrated in ReaDDy and can be used. The concentrations over time for this reaction results in:

$$c_S(t) = c_{s_0} e^{-tk_1 c_E} \tag{3.3}$$

$$c_P(t) = c_{s_0}\left(1 - e^{-tk_1 c_E}\right) \tag{3.4}$$

for boundary conditions $c_P(0) = 0$. The intrinsic reaction parameter is set to be infinite so that reactions occur immediately if particles surpass the reaction radius σ. This setup is completely diffusion limited and eq. (3.1) can be applied. The

resulting time dependent concentrations are:

$$c_S(t) = c_{s_o} e^{-t4\pi(D_1+D_2)\sigma c_E} \tag{3.5}$$

$$c_P(t) = c_{s_0}\left(1 - e^{-t4\pi(D_1+D_2)\sigma c_E}\right) \tag{3.6}$$

This setup has been simulated with only one enzyme. The time dependent particle number of the substrate $S(t)$ was recorded for different diffusion constants and compared to the theoretical values. The result can be seen in fig. 3.1. The theory is fitting to the exponential decay in the simulation. This simulation shows the influence of D on reactions.

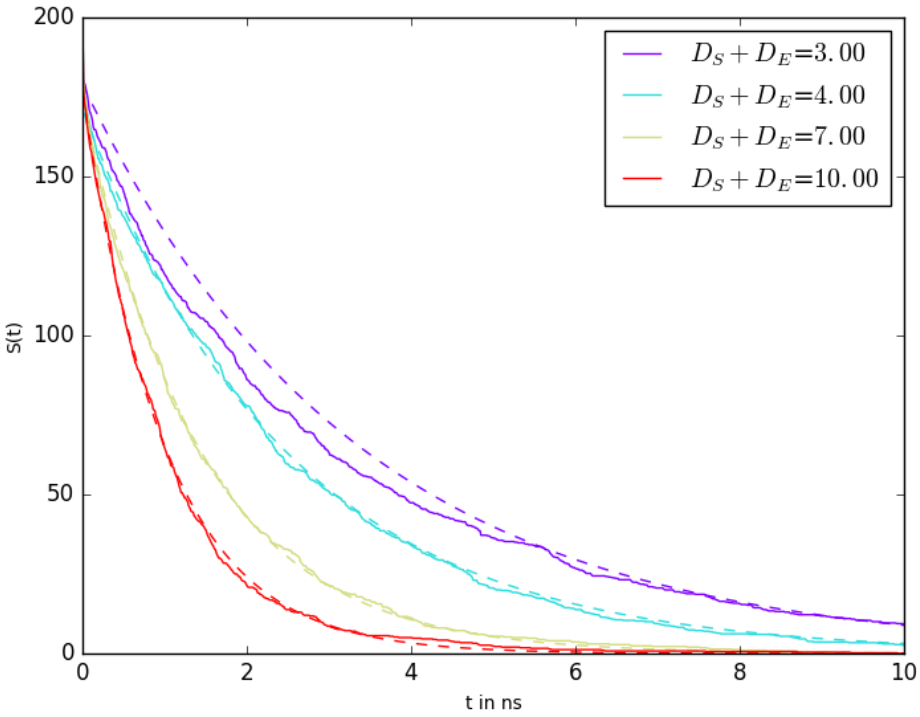

Figure 3.1: Substrate particle number $S(t)$ for different Diffusion constants D of the enzyme and substrate. With fitted theoretical curves from equation eq. (3.5). The input parameters for RevReaDDy are: box size= $10^3 nm$,reaction distance = 3,intrinsic reaction rate= 10^{25}, timesteps= 1000,$S(0) = 300$.

In the second half of the master thesis fBm is going to be integrated in RevReaDDy. Similar simulations with fBm are going to be studied and related to Brownian motion. Spatial distributions of the reactants are going to be studied. The algorithm for fBm uses his velocity autocorrelation function. In principle it should be possible to integrate also different VACFs. The fBm integrator would result in an more

general integrator, which could be used to model environments from real experiments. Including the VACF in the integrator may be an elegant way of adding an approximation due to the experimental environment.

4 Appendix

4.1 From Central Limit Theorem to Gaussian Distribution

In the following the Central Limit Theorem will be applied to calculated the distribution of Y, $\rho(y)dy = P(y < Y < y + dy)$ in the limit of large N , with Y being defined as the sum of an random variable:

$$Y = \frac{1}{\sqrt{N}} \sum_{j=1}^{N} X_j \tag{4.1}$$

The Generating function for a random variable Y is:

$$G_Y(k) = \langle e^{ikY} \rangle = \int e^{ikY} \rho(y) dy \tag{4.2}$$

eq. (4.1) can be inserted into the generating function, which results in:

$$G_Y(k) = \langle e^{\frac{ik}{\sqrt{N}} \sum_{j=1}^{N} X_j} \rangle$$

$$G_Y(k) = \langle \prod_{j=i}^{N} e^{\frac{ik}{\sqrt{N}} X_j} \rangle$$

If all X_j are independent, then:

$$G_Y(k) = \prod_{j=i}^{N} \langle e^{\frac{ik}{\sqrt{N}} X_j} \rangle = e^{\sum_{j=1}^{N} A_j(\frac{k}{\sqrt{N}})} \tag{4.3}$$

$$\text{with } A_j(\frac{k}{\sqrt{N}}) = ln \langle e^{\frac{ik}{\sqrt{N}} X_j} \rangle$$

For large N behavior, we assume $\frac{k}{\sqrt{N}} << 1$ and expand

$$A_j(\frac{k}{\sqrt{N}}) = ln(1 + \langle X_j \rangle \frac{ik}{\sqrt{N}} - \langle X_j^2 \rangle \frac{k^2}{2N} + \mathcal{O}(N^{-\frac{3}{2}})) \tag{4.4}$$

with a finite variance $\sigma_i^2 = \langle X_i^2 \rangle$ and the mean $\langle X_i \rangle = 0$

$$A_j(\frac{k}{\sqrt{N}}) = -\sigma_j^2 \frac{k^2}{2N} + \mathcal{O}(N^{-\frac{3}{2}})) \tag{4.5}$$

Thus, the generating function for large N is:

$$G_Y(k) = e^{-\frac{\sigma^2 k^2}{2}} \tag{4.6}$$
$$\text{with } \sigma = \frac{1}{N}\sum_{j=1}^{N}\sigma_j^2$$

The distribution of Y can be calculated via the inverse Fourier Transform:

$$\rho(y) = \frac{1}{2\pi}\int_{-\infty}^{\infty} e^{-\frac{\sigma^2 k^2}{2}} e^{iky} dk \tag{4.7}$$
$$= \frac{1}{\sqrt{2\pi}\sigma} e^{-\frac{y^2}{2\sigma^2}} \tag{4.8}$$

$\rho(y)$ results in a Gaussian distribution.

4.2 From Gaussian Distribution to Gaussian Transition Probability

The conditional distribution function to be in x at time t if visited position y at time s can be written due to Bayes' theorem as a transition probability from y to x in time $t - s$ multiplied with the probability to be in y at time s:

$$\rho_{t,s}(x, y) = T_{t-s}(x|y)\rho_s(y) \tag{4.9}$$

Further due to particle conservation another relation holds:

$$\rho_t(x) = \int \rho_{t,s}(x, y) dy \tag{4.10}$$

Having an initial condition $\rho_s(x) = \delta(x - y)$:

$$\rho_{t,s}(x|y) = \int \rho_{t,s}(x, y) dy = \int T_{t-s}(x|y)\rho_s(y) dy \tag{4.11}$$
$$= \int T_{t-s}(x|y)\delta(x - y) dy = T_{t-s}(x|y) \tag{4.12}$$

4.3 Einstein Formula

The derivative of the mean variance of the Gaussian distribution in respect to time is defined as:

$$\frac{d}{dt}\delta\boldsymbol{r}^2(t) = \frac{d}{dt}\langle\Delta\boldsymbol{R}^2(t)\rangle = \frac{d}{dt}\int d\boldsymbol{r}\boldsymbol{r}^2 c(\boldsymbol{r}, t) = \int d\boldsymbol{r}\boldsymbol{r}^2 \frac{\partial}{\partial t} c(\boldsymbol{r}, t) \tag{4.13}$$

Fick's second law can be applied:

$$= D \int_{-\infty}^{\infty} d\boldsymbol{r} \boldsymbol{r}^2 \Delta c(\boldsymbol{r}, t) \tag{4.14}$$

Assuming a reasonable assumption $c(\pm\infty, t) = 0$ and two times partial integration one can derive:

$$= -2D \int_{-\infty}^{\infty} d\boldsymbol{r} \boldsymbol{r} \nabla c(\boldsymbol{r}, t) \tag{4.15}$$

$$= 2Dd \int_{-\infty}^{\infty} d\boldsymbol{r} c(\boldsymbol{r}, t) = 2dD \tag{4.16}$$

For the initial condition $\boldsymbol{r}(0) = 0$, one gets the Einstein Formula: $\langle (\boldsymbol{r}(t) - \boldsymbol{r}(0))^2) \rangle = 2dDt$

4.4 Autocorrelation Function for fBm

Subsequently, the VACF in the frequency domain for Fractional Brownian motion can be calculated. The MSD is $\delta r^2(t) =< \Delta R(t) >= 2dK_\alpha t^\alpha$ with K_α being the generalized diffusion-coefficient:

$$\begin{aligned} \tilde{Z}(z) &= \int_0^\infty dt e^{izt} Z(t) \\ &= \frac{1}{2d} \int_0^\infty dt e^{izt} \left[\frac{d^2}{dt^2} \delta r^2(t) \right] \end{aligned}$$

Partial integration:

$$\overset{par.integ.}{=} \frac{1}{2d} \left(\underbrace{\left[e^{izt} \overbrace{\frac{d}{dt} 2dK_\alpha t^\alpha}^{=A(t)} \right]_0^\infty}_{\overset{\alpha \leq 2}{=} 0} - iz \int_0^\infty dt e^{izt} \left[\frac{d}{dt} \delta r^2(t) \right] \right)$$

$$A(t) = \frac{d}{dt} \overbrace{\left[\frac{2dK_\alpha t^{\alpha-1}}{\alpha} \right]}^{B(t)} = \frac{2dK_\alpha t^{\alpha-2}}{\alpha + (\alpha - 1)}$$

Partial integration and Tauber theorem:

$$\tilde{Z}(z) \overset{par.integ.}{=} -\frac{1}{2d}\left(\underbrace{\left[e^{izt}\overbrace{2dK_\alpha t^\alpha}^{=B(t)}\right]_0^\infty}_{\overset{\alpha\leq 1}{=}0} - (iz)^2\int_0^\infty dt e^{izt}\delta r^2(t)\right)$$
$$= -\frac{z^2}{2d}\int_0^\infty dt e^{izt}\delta r^2(t) \overset{\mathrm{Im}(z)>0}{=} K_\alpha\Gamma(1+\alpha)(iz)^{1-\alpha}$$

4.5 Kinetics of the Bi-Molecular Chemical Reaction in Solution

The aim of this calculation is to derive the kinetics for the following reaction scheme:
$\mathrm{A} + \mathrm{B} \underset{k_\mathrm{d}^-}{\overset{k_\mathrm{d}^+}{\rightleftharpoons}} \mathrm{AB}$
The derivation is calculated under the assumption of free diffusion of particle A and B with the diffusion constants D_A and D_B , respectively and without any interactions between them. The joint concentration field can be described by the Smoluchowski equation for a bi-molecular system in a solution:

$$\frac{\partial\rho_t(\boldsymbol{r}_A,\boldsymbol{r}_B)}{\partial t} = (D_A\nabla_A^2 + D_B\nabla_B^2)\rho_t(\boldsymbol{r}_A,\boldsymbol{r}_B) \tag{4.17}$$

The complexity of the problem can be reduced by substituting the positions of the particles A and B with their relative distance $\boldsymbol{r} = \boldsymbol{r}_A - \boldsymbol{r}_B$. It is convenient to introduce even further substitutions:

$$D = D_A + D_B \qquad \boldsymbol{R} = \frac{D_B\boldsymbol{r}_A + D_A\boldsymbol{r}_B}{D_A + D_B} \tag{4.18}$$

the Laplace operator in terms of new coordinates result in:

$$\nabla_A^2 = \left(\nabla_r + \frac{D_B}{D}\nabla_R\right)^2 \tag{4.19}$$

$$\nabla_B^2 = \left(\nabla_r + \frac{D_A}{D}\nabla_R\right)^2 \tag{4.20}$$

Inserting these in eq. (4.17) one gets:

$$\frac{\partial\tilde{\rho}_t(\boldsymbol{r},\boldsymbol{R})}{\partial t} = \left(D\nabla_r^2 + \frac{D_BD_A}{D_A+D_B}\nabla_R^2\right)\tilde{\rho}_t(\boldsymbol{r},\boldsymbol{R}) \tag{4.21}$$

The equation is describing two independent diffusion processes, one in the coordinate $\boldsymbol{r}$ and one in the coordinate $\boldsymbol{R}$. The solution can be obtained by the product ansatz

$\tilde{\rho}_t(\boldsymbol{r}, \boldsymbol{R}) = \rho_t(\boldsymbol{r})q_t(\boldsymbol{R})$. Integration over $\boldsymbol{R}$ results in:

$$\frac{\partial \rho_t(\boldsymbol{r})}{\partial t} = D\nabla_r^2 \rho_t(\boldsymbol{r}) + \frac{D_B D_A}{D_A + D_B} \nabla_R^2 \rho_t(\boldsymbol{r}) \int_{\partial V} q_t(\boldsymbol{R}) d\boldsymbol{a} \tag{4.22}$$

In the previous equation the stokes theorem was applied. The second term is zero due to conservation of probability. The problem is isotropic, hence $r = |\boldsymbol{r}|$ and $\nabla_{\boldsymbol{r}}^2 = \left(\partial_r + \frac{2}{r}\right)\partial$. The equation reduce to one dimension:

$$\frac{\partial \rho_t(r)}{\partial t} = -\left(\frac{\partial}{\partial_r} + \frac{2}{r}\right) j_t(r) \qquad j_t(r) = D\frac{\partial \rho_t(r)}{\partial_r} \tag{4.23}$$

The stationary distribution results in:

$$0 = -\left(\frac{\partial}{\partial_r} + \frac{2}{r}\right) j_t^s(r) \tag{4.24}$$

$$\frac{dj_t^s(r)}{j_t^s(r)} = -\frac{2}{r}dr \tag{4.25}$$

$$j_t^s(r) = Ar^{-2} \tag{4.26}$$

$$\rho^s(r) = \rho^s(r_0) - \frac{\int_{r_0}^r j_t^s(r')dr'}{D} = \rho^s(r_0) + \frac{A}{D}\left(\frac{1}{r} - \frac{1}{r_0}\right) \tag{4.27}$$

Now assuming only a single B molecule being at the position $r = 0$. Instantaneous reaction occur for $r \leq \sigma \Rightarrow \rho_t(r \leq \sigma) = 0$. For $r \to \infty$ the distribution is than defined as the concentration of particle A $\rho_t(r \to \infty) = c_A$ and the Solutions for $\rho^s(r)$ and $j_t^s(r)$ for the boundary conditions are:

$$\rho^s(r) = C_A\left(1 - \frac{\sigma}{r}\right) \qquad j_t^s(r) = -D\sigma C_A r^{-2} \tag{4.28}$$

The change of the concentration of C_{AB} is then:

$$\frac{dC_{AB}}{d} = 4\pi\sigma D C_A C_B \tag{4.29}$$

By formulating the problem in relative distance from particle A and B. It was also reasonable to keep particle B at its initial position. The results shows the relation between the product of the concentrations and the concentration change.In the derivation of Michealis-Menten kinetics this is an assumption.

4.6 Michaelis-Menten Kinetics

Michaelis-Menten kinetics are describing the following system:
$\mathrm{S} + \mathrm{E} \underset{k_1'}{\overset{k_1}{\rightleftarrows}} \mathrm{ES} \xrightarrow{k_2} \mathrm{P} + \mathrm{E}$. A range of differential equations can be formulated as a result of particle conservation and the assumption for a bi-molecular chemical

reaction to be proportional to the product of the reactants concentration.

$$\frac{d[P]}{dt} = k_2[ES] \tag{4.30}$$

$$\frac{d[E]}{dt} = k_2[ES] + k_1'[ES] - k_1'[E][S] \tag{4.31}$$

$$\frac{d[S]}{dt} = k_1'[ES] - k_1'[E][S] \tag{4.32}$$

$$\frac{d[ES]}{dt} = -k_2[ES] - k_1'[ES] + k_1'[E][S] \tag{4.33}$$

With a quasi-steady-state approximation: $\frac{d[ES]}{dt} = 0 \longrightarrow k_1[E][S] = k_1'[ES]+k_2[ES]$. A Rearrangement of this equation results in the Michaelis-Menten constant: $K_M = \frac{k_1'+k_2}{k_1} = \frac{[E][S]}{[ES]}$. From the enzyme conservation law one gets:

$$[E] = [E]_0 - [ES] \tag{4.34}$$

After inserting eq. (4.34) into the quasi-steady-state approximation, one gets:

$$[ES] = \frac{[E]_0[S]}{K_M + [S]} \tag{4.35}$$

Combining it with the first differential eq. (4.31) one gets the rate of Product production:

$$v = \frac{d[P]}{dt} = k_2\frac{[E]_0[S]}{K_M + [S]} = V_{max}\frac{[S]}{K_M + [S]} \tag{4.36}$$

Bibliography

[1] Hugues Berry.
Monte carlo simulations of enzyme reactions in two dimensions: fractal kinetics and spatial segregation.
Biophysical journal, 83(4):1891–1901, 2002.

[2] Peter F. Craigmile.
Simulating a class of stationary Gaussian processes using the Davies-Harte algorithm, with application to long memory processes.
Journal of Time Series Analysis, 24(5):505–511, 2003.

[3] Höfling Felix.
Stochastic processes and correlation functions.
University Lecture, 2016.

[4] Mark B Flegg.
Smoluchowski reaction kinetics for reactions of any order.
pages 1–30.

[5] S Havlin and D Ben Avraham.
Diffusion in Disordered Media.
Advances in Physics, 36:695–798, 1987.

[6] Felix Höfling and Thomas Franosch.
Anomalous transport in the crowded world of biological cells.
Reports on Progress in Physics, 76(4):046602, apr 2013.

[7] J. R. M. Hosking.
Modeling persistence in hydrological time series using fractional differencing.
Water Resources Research, 20(12):1898–1908, 1984.

[8] Kenneth A. Johnson and Roger S. Goody.
The original Michaelis constant: Translation of the 1913 Michaelis-Menten Paper.
Biochemistry, 50(39):8264–8269, 2011.

[9] Benoit B. Mandelbrot and John W. Van Ness.
Fractional Brownian Motions, Fractional Noises and Applications.
SIAM Review, 10(4):422–437, oct 1968.

[10] Allen P Minton.
How can biochemical reactions within cells differ from those in test tubes?
Journal of cell science, 119(Pt 14):2863–9, 2006.

[11] Johannes schöneberg.
REACTION-DIFFUSION DYNAMICS IN BIOLOGICAL SYSTEMS.

PhD thesis, 2014.

[12] M. v. Smoluchowski.
Versuch einer mathematischen Theorie der Koagulationskinetik kolloider Lösungen.

[13] Huan-Xiang Zhou, Germán Rivas, and Allen P Minton.
Macromolecular crowding and confinement: biochemical, biophysical, and potential physiological consequences.
Annual review of biophysics, 37:375–97, 2008.